J Arid Land (2023) 15(1): 91–108
https://doi.org/10.1007/s40333-022-0079-8

Science Press Springer-Verlag

Quantitative distinction of the relative actions of climate change and human activities on vegetation evolution in the Yellow River Basin of China during 1981–2019

LIU Yifeng[1], GUO Bing[1,2,3,4,5*], LU Miao[6*], ZANG Wenqian[4,7], YU Tao[4,7,8], CHEN Donghua[8]

[1] School of Civil Architectural Engineering, Shandong University of Technology, Zibo 255000, China;
[2] Key Laboratory of Urban Land Resources Monitoring and Simulation, Ministry of Natural Resources, Shenzhen 518000, China;
[3] Key Laboratory of National Geographic Census and Monitoring, Ministry of Natural Resources, Wuhan 430072, China;
[4] Aerospace Information Research Institute, Chinese Academy of Sciences, Beijing 100101, China;
[5] State Key Laboratory of Resources and Environmental Information System, Institute of Geographic Sciences and Natural Resources Research, Chinese Academy of Sciences, Beijing 100101, China;
[6] Key Laboratory of Agricultural Remote Sensing, Ministry of Agriculture and Rural Affairs/Institute of Agricultural Resources and Regional Planning, Chinese Academy of Agricultural Sciences, Beijing 100081, China;
[7] Zhongke Langfang Institute of Spatial Information Applications, Langfang 065000, China;
[8] College of Computer and Information Engineering, Chuzhou University, Chuzhou 239000, China

Abstract: Under the combined influence of climate change and human activities, vegetation ecosystem has undergone profound changes. It can be seen that there are obvious differences in the evolution patterns and driving mechanisms of vegetation ecosystem in different historical periods. Therefore, it is urgent to identify and reveal the dominant factors and their contribution rates in the vegetation change cycle. Based on the data of climate elements (sunshine hours, precipitation and temperature), human activities (population intensity and GDP intensity) and other natural factors (altitude, slope and aspect), this study explored the spatial and temporal evolution patterns of vegetation NDVI in the Yellow River Basin of China from 1989 to 2019 through a residual method, a trend analysis, and a gravity center model, and quantitatively distinguished the relative actions of climate change and human activities on vegetation evolution based on Geodetector model. The results showed that the spatial distribution of vegetation NDVI in the Yellow River Basin showed a decreasing trend from southeast to northwest. During 1981–2019, the temporal variation of vegetation NDVI showed an overall increasing trend. The gravity centers of average vegetation NDVI during the study period was distributed in Zhenyuan County, Gansu Province, and the center moved northeastwards from 1981 to 2019. During 1981–2000 and 2001–2019, the proportion of vegetation restoration areas promoted by the combined action of climate change and human activities was the largest. During the study period (1981–2019), the dominant factors influencing vegetation NDVI shifted from natural factors to human activities. These results could provide decision support for the protection and restoration of vegetation ecosystem in the Yellow River Basin.

Keywords: vegetation evolution; driving mechanisms; climate change; human activities; relative actions; Geodetector; Yellow River Basin

*Corresponding authors: GUO Bing (E-mail: guobingjl@163.com); LU Miao (E-mail: lumiao@caas.cn)
Received 2022-07-05; revised 2022-09-05; accepted 2022-09-14

Citation: LIU Yifeng, GUO Bing, LU Miao, ZANG Wenqian, YU Tao, CHEN Donghua. 2023. Quantitative distinction of the relative actions of climate change and human activities on vegetation evolution in the Yellow River Basin of China during 1981–2019. Journal of Arid Land, 15(1): 91–108. https://doi.org/10.1007/s40333-022-0079-8

1 Introduction

Terrestrial ecosystems are an important part of the global ecosystem, which are more sensitive to the process of climate change (Hou et al., 2022). As the main body of terrestrial ecosystems, the dynamic coupling between vegetation and climate has a profound impact on terrestrial ecosystems (Zhang et al., 2022). Moreover, vegetation is extremely sensitive to climate change, so the dynamic of vegetation change is often used as a biological indicator of global climate change (Wang et al., 2008; Guo et al., 2020a; Jiang et al., 2021; Zhang et al., 2022). With the intensification of global climate research, the relationships between vegetation change and climate change have become one of the core foci of ecological research (Yuan et al., 2022).

In recent years, a series of studies on vegetation monitoring, spatial and temporal distribution of vegetation, vegetation evolution processes and the driving mechanisms have been carried out by domestic and foreign scholars (e.g., Fang et al., 2021; Wu et al., 2021; Stecca et al., 2022). Zhong et al. (2010) investigated the spatial and temporal patterns of vegetation in the Qinghai-Tibet Plateau of China during 1998–2006 and found that the spatial distribution of vegetation NDVI was consistent with the climatic pattern. Wu et al. (2014) found that the annual variation of global average vegetation coverage fluctuated in the range of 0.2–0.6. Duo et al. (2016) analyzed the vegetation changes in the North China Plain at different spatial (forests, grasslands, etc.) and temporal (years, seasons and months) scales and indicated that zones with an increasing trend of vegetation coverage accounted for 55.000% of the North China Plain. Morgan et al. (2020) pointed out that there was an overall increase of 33.000% in vegetation coverage in large shallow rivers during 1984–2019, based on Unmanned Aerial Vehicle (UAV) and Landsat images. In addition to the above research projects, in recent years, Chinese scholars have also studied vegetation coverage change in the Qinghai-Tibet Plateau, the Qinba Mountains, the North China Plain, the Lancang River Basin and the Loess Plateau in China, revealing the stages and regional differences of vegetation coverage change in China (e.g., Dai et al., 2014; Qiao et al., 2020; Sidi et al., 2021). Vegetation evolution is often comprehensively influenced by many factors, such as precipitation, topography, temperature and human activities. For example, Yi et al. (2014) utilized the Systeme Probatoire d'Observation de la Terre (SPOT) vegetation data to investigate the influences of climate change and human activities on vegetation coverage change in the Loess Plateau, and revealed that precipitation played an important role in affecting vegetation coverage change, while human activities exhibited a positive impact on vegetation Normalized Difference Vegetation Index (NDVI). Lu et al. (2021) suggested that strong precipitation had significant positive influences on vegetation in the growing season. Based on the remote sensing data of the Advanced Very High-Resolution Radiometer (AVHRR) leaf area index, Li et al. (2022) analyzed the spatial and temporal distribution characteristics of vegetation coverage in the Yellow River Basin, and discussed the impact and contribution rate of climate elements on the change of vegetation coverage. Wang et al. (2022) used the remote sensing cloud computing platform of the Google Earth Engine (GEE) to invert the fractional vegetation cover of the Yellow River Basin from 1999 to 2019 through a pixel dichotomous model and then investigated the driving mechanisms of vegetation coverage change by Geodetector model. Chen et al. (2022) revealed that precipitation was the dominant factor in the change process of vegetation NDVI in semi-arid regions of the Yellow River Basin, while temperature exhibited the greatest contribution rate to the change of vegetation NDVI in humid regions of the basin.

The Yellow River Basin, with a vast area, has an extremely important strategic position in national development of China (Chen et al., 2021; Lu et al., 2021; Zhu and Zhang, 2022). On 18 September 2019, the importance of protecting the ecological environment of the Yellow River Basin was stressed at the Symposium on Ecological Protection and High-quality Development

(Qu et al., 2020; Meng et al., 2022). Under the combined influence of climate change and human activities, the problems of soil erosion and vegetation degradation in the Yellow River Basin have become prominent (Tardy et al., 2005; Agatova et al., 2020). In different historical periods, there are significant differences in the evolution patterns and driving mechanisms of vegetation ecosystem (Oakley et al., 2018; Zhang et al., 2022). Whether the problems are caused by climate change or human activities, or a combination of both, and what are the contribution rate and the nature of the differences between the two, are still unclear (Guo et al., 2020b; Wu et al., 2022). Therefore, it is an urgent matter to distinguish the relative actions of climate change and human activities on vegetation evolution and clarify the dominant factors in different historical periods, which can provide decision-making support for the precise restoration of vegetation in the Yellow River Basin (Amundson et al., 2015; Guo et al., 2022a).

Therefore, based on the meteorological data, Global Inventor Modeling and Mapping Studies Normalized Difference Vegetation Index (GIMMS NDVI) and Moderate Resolution Imaging Spectrometer Normalized Difference Vegetation Index (MODIS NDVI) data in the Yellow River Basin from 1981 to 2019, this study investigated and explored the spatial and temporal evolution patterns of vegetation NDVI change in the basin using a residual method, a trend analysis, and a gravity center model, and then quantitatively distinguished the relative actions of climate change and human activities on vegetation evolution using Geodetector model, and finally revealed the dominant factors of vegetation evolution in different historical periods. This study could provide a method reference for quantitatively distinguishing the relative actions of climate change and human activities on the spatial and temporal evolution patterns of vegetation NDVI, supporting for ecological conservation activities and high-quality development of the Yellow River Basin.

2 Materials and methods

2.1 Study area

The Yellow River originates from the Bayan Har Mountains, bordering the Bohai Sea in the west, the Qinling Mountains in the north and the Yinshan Mountains in the south, with an area of 79.45×10^4 km^2 (32°–42°N, 96°–119°E; Fig. 1). The elevation of the Yellow River Basin ranges from 10 to 6255 m. The terrain in the basin shows a decreasing trend from west to east, forming a three-stage ladder from west to east. Heyuan Town to Hekou Town in Inner Mongolia Autonomous Region forms the upper reaches of the basin, which is characterized by high mountains and wide distribution of woodland. The middle reaches of the basin from Hekou Town in Inner Mongolia Autonomous Region to Peach blossom valley in Henan Province are dominated by the Inner Mongolia Plateau and the Loess Plateau with serious soil and water erosion. Most areas of the basin are characterized by arid and semi-arid climate, and water resources are consistent deficient. The lower reaches of the Yellow River has a length of about 786 km, with flat terrain. Temperature shows obvious regional differences in the basin, with an annual average temperature of 2.7°C. Precipitation exhibits a deceasing trend from southeast to northwest, with an average annual precipitation of less than 450.0 mm. The eco-environment in the Yellow River Basin is vulnerable to climate change and human activities, with severe soil erosion, frequent droughts and serious vegetation degradation.

2.2 Data and processing

The datasets utilized in this study were mainly composed of climate elements (including annual average temperature, annual precipitation and annual sunshine hours), human activity factors (including GDP intensity and population intensity) (Ling et al., 2006; Zhao et al., 2021), other natural factors (including aspect, altitude and slope), and vegetation NDVI data. The annual average temperature (the ratio of sum of the daily temperature and days to 0.1°C), annual precipitation (sum of daily precipitation to 0.1 mm) and annual sunshine hours (sum of daily sunshine hours to 0.1 h) during 1981–2019 were obtained from the China Meteorological Data

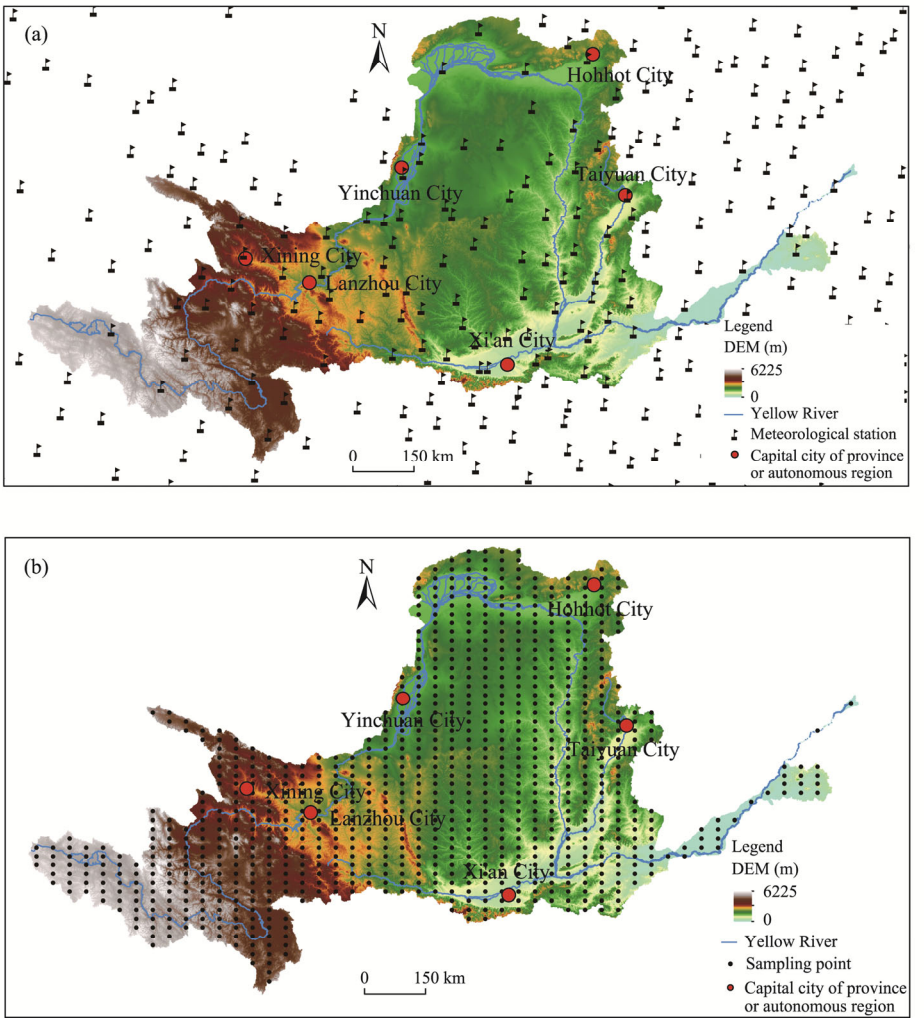

Fig. 1 Overview of the Yellow River Basin based on digital elevation model (DEM) data. (a), spatial distribution of meteorological stations; (b), spatial distribution of sampling points of Normalized Difference Vegetation Index (NDVI).

Service Centre (http://data.cma.cn/). GDP intensity and population intensity data were from the study of Ling et al. (2006). We obtained the slope and aspect datasets with the spatial resolution of 1 km based on digital elevation model (DEM) data downloaded from the Geospatial Data Cloud (http://www.gscloud.cn) using tools in the 3D Analyst tool in ArcGIS. The vegetation NDVI datasets used in this study included GIMMS NDVI (1981–2000) and MODIS NDVI (2001–2019).

GIMMS NDVI is produced by the NASA Land Data Centers with the spatial and temporal resolutions of 8 km and 15 d, respectively. MODIS NDVI derived from MOD13A3 was downloaded from the Geospatial Data Cloud (http://www.gscloud.cn) with the spatial resolution of 1 km and temporal resolution of 16 d. In order to confirm the consistency of temporal and spatial resolutions, we resampled the NDVI data from 8 to 1 km based on bilinear interpolation and re-projected the data from WGS 1984 to Krasovsky_1940_Albers, and then calculated the maximum value composite. In addition, due to the difference between the two sensors, the data correction should be applied to confirm the comparability among two datasets. The sampling points were obtained by the uniform distribution method for the verification of NDVI, with a total of 901 sampling points, as shown in Figure 1b. In this study, the function of the sampling

points was used to verify the accuracy of NDVI data, with R^2=0.925 and P<0.001. The fitting equation is as follows:

$$y = 1.0777x + 0.0046, \quad (1)$$

where x is the GIMMS NDVI and y is the MODIS NDVI.

As shown in Figure 1, there are 235 meteorological stations in and around the Yellow River Basin. The meteorological stations in the Yellow River Basin (175 stations) were applied for Kriging interpolation, while the remaining stations (60 stations) were used for the accuracy validation of interpolation results. The overall accuracies of interpolation results for annual average temperature, annual precipitation and annual sunshine hours were 91.6%, 92.3% and 90.5%, respectively, which satisfied the needs of this study. The Kriging interpolation method of ArcGIS 10.4 was applied to obtain the grids of annual average temperature, annual precipitation and annual sunshine hours with a spatial resolution of 1 km from 1981 to 2019.

2.3 Methods

2.3.1 Residual method

The NDVI residual method is widely applied to quantitatively distinguish the impacts of climate change and human activities on vegetation coverage change (Liu et al., 2021). The related equations are as follows:

$$NDVI_{human} = NDVI_{actual} - NDVI_{climate}, \quad (2)$$

$$NDVI_{climate} = \alpha \times P + \beta \times T + \delta \times S + \varphi, \quad (3)$$

where $NDVI_{actual}$ is the observed vegetation NDVI value by remote sensing images, which is the result of the combined action of climate change and human activities; $NDVI_{climate}$ is the predicted vegetation NDVI value by regression analysis, which is the action result of climate change; $NDVI_{human}$ is the residual value of $NDVI_{actural}$ and $NDVI_{climate}$, which is the action result of human activities; α is the regression coefficient between vegetation NDVI and precipitation; P is the annual precipitation (mm); β is the regression coefficient between vegetation NDVI and temperature; T is the annual average temperature (°C); δ is the regression coefficient between vegetation NDVI and sunshine hours; S is the annual sunshine hours (h); and φ is a regression constant.

2.3.2 Linear regression method and change intensity of vegetation NDVI

Trend analysis works to analyze the intensity of vegetation coverage change in the region by linear regression (Twilley et al., 2019). The calculation formula is as follows:

$$K = \frac{n \times \sum_{i=1}^{n} (i \times Y_{NDVI,i}) - \sum_{i=1}^{n} \sum_{i=1}^{n} Y_{NDVI,i}}{n \times \sum_{i=1}^{n} i^2 - \left(\sum_{i=1}^{n} i \right)^2}, \quad (4)$$

where K is the gradient of the trend line; n is the total number of sequential years (n=39); and $Y_{NDVI,i}$ is the maximum vegetation NDVI in year i. When K>0, it means that the vegetation condition is improved, and vice versa.

We obtained the change intensity of vegetation NDVI during 1981–2019 by the extraction method, and classified the change intensity based on the histogram distribution and standard deviation of the images.

2.3.3 Gravity center model

The gravity center model can characterize the spatial bias and deviation of geographical elements, which is widely used in social, economic and ecological fields. If a region consists of m sub-regions (where the gravity coordinates of sub-region j are expressed as (x_j, y_j)) and M_j refers to the attribute value of the sub-region, then the geographical coordinate $(\bar{x}, \bar{y})$ of the regional gravity centers is expressed as follows:

$$\bar{x}=\frac{\sum_{j=1}^{m}M_j x_j}{\sum_{j=1}^{m}M_j},\quad \bar{y}=\frac{\sum_{j=1}^{m}M_j y_j}{\sum_{j=1}^{m}M_j}. \tag{5}$$

2.3.4 Geodetector model

Geodetector model can be utilized to investigate the spatial differentiation patterns of vegetation NDVI and determine the dominant influencing factors on vegetation NDVI measured by the q value (ranging from 0 to 1). The correlation degree is represented by the q value, and the explanatory power of a factor to vegetation NDVI can be revealed. The larger the q value is, the higher the explanatory power of this factor to vegetation NDVI is, and vice versa. The equations are as follows:

$$q=1-\frac{\sum_{h=1}^{L}N_h\sigma_h^{\ 2}}{N\sigma^2}=1-\frac{SSW}{SST}, \tag{6}$$

$$SSW=\sum_{h=1}^{L}N_h\sigma_h^{\ 2}, \tag{7}$$

$$SST=N\sigma^2, \tag{8}$$

where SSW represents the sum of intra-layer variance; SST refers to the total variance of the whole region; h is the classification of variable or factor (h=1, 2, ..., L); N_h is the number of units of class h; N is the number of units of the whole region; σ_h is the variance of variable of class h; and σ is the variance of variable of the whole region.

2.3.5 Relative action distinctions of climate change and human activities on vegetation NDVI

Vegetation NDVI in the Yellow River Basin is comprehensively affected by climate change and human activities, and the relative actions of the above two on vegetation evolution could be evaluated by the changes of vegetation NDVI. In this paper, the linear regression method (Eq. 4) was applied to calculate the change gradients of $NDVI_{climate}$, $NDVI_{human}$ and $NDVI_{actural}$ in the Yellow River Basin from 1981 to 2019. K_A, K_C and K_H were used to indicate the change trends of $NDVI_{actural}$, $NDVI_{climate}$, and $NDVI_{human}$, respectively. According to Table 1, the relative actions of climate change and human activities on vegetation evolution in the Yellow River Basin from 1981 to 2019 were divided into six scenarios: vegetation restoration promoted by the combined action of climate change and human activities as scenario 1; vegetation restoration promoted by climate change as scenario 2; vegetation restoration promoted by human activities as scenario 3; vegetation degradation induce by the combined action of climate change and human activities as scenario 4; vegetation degradation induce by climate change as scenario 5; and vegetation degradation induce by human activities as scenario 6.

Table 1 Relative action distinctions of climate change and human activities on vegetation evolution

Vegetation evolution	Scenario	K_C	K_H	Contribution of climate change (%)	Contribution of human activities (%)
Vegetation restoration (K_A>0)	1	>0	>0	Combined action	Combined action
	2	>0	<0	100.000	0.000
	3	<0	>0	0.000	100.000
Vegetation degradation (K_A<0)	4	<0	<0	Combined action	Combined action
	5	<0	>0	100.000	0.000
	6	>0	<0	0.000	100.000

Note: K_A, K_C and K_H were used to indicate the change trends of $NDVI_{actural}$, $NDVI_{climate}$, and $NDVI_{human}$, respectively. NDVI, Normalized Difference Vegetation Index. $NDVI_{actual}$ is the observed vegetation NDVI value by remote sensing images, which is the result of the combined action of climate change and human activities; $NDVI_{climate}$ is the predicted vegetation NDVI value by regression analysis, which is the action result of climate change; $NDVI_{human}$ is the residual value of $NDVI_{actural}$ and $NDVI_{climate}$, which is the action result of human activities.

3 Results

3.1 Spatial distribution of average vegetation NDVI during 1981–2019

The spatial distribution of average vegetation NDVI during 1981–2019 was analyzed in this study. Figure 2 showed that average vegetation NDVI in the Yellow River Basin fluctuated between –0.40 and 0.92. Zones with lower vegetation NDVI values were mainly distributed in Ordos City in Inner Mongolia Autonomous Region, Wuzhong City and Zhongwei City in northern Ningxia Hui Autonomous Region, and Baiyin City and Lanzhou City in northern Gansu Province. Zones with higher vegetation NDVI values were mainly located in Huangnan Tibetan Autonomous Prefecture in western Qinghai Province and Gannan Tibetan Autonomous Prefecture in southwestern Gansu Province.

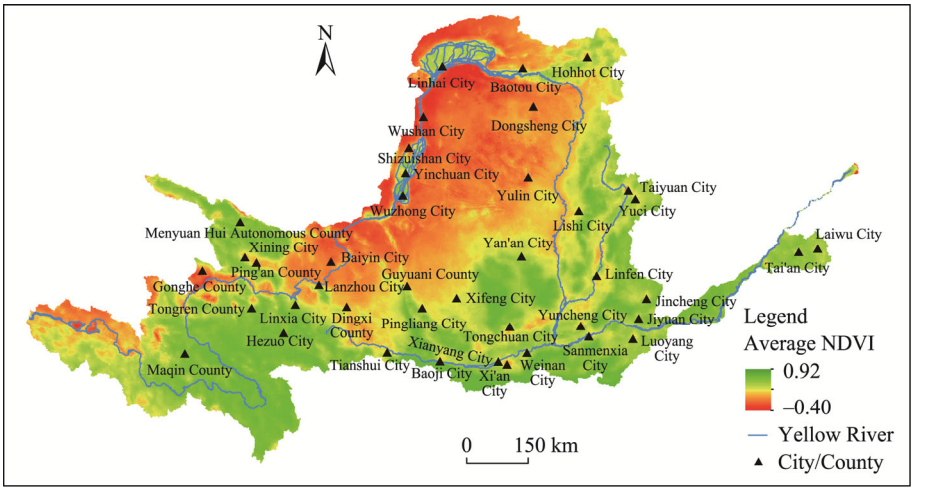

Fig. 2 Spatial distribution of average Normalized Difference Vegetation Index (NDVI) in the Yellow River Basin during 1981–2019

3.2 Spatial distribution of NDVI change intensity during 1981–2019

In order to more intuitively reflect the spatial distribution of NDVI change intensity in the Yellow River Basin during 1981–2019, we classified NDVI change intensity according to the standard deviation of the distribution histogram (Lu et al., 2022). NDVI change intensity in the Yellow River Basin during 1981–2019 was analyzed, and the results showed that zones with a slight increase in vegetation NDVI had the largest area, accounting for 63.830% of the total basin area, indicating that the vegetation condition in most areas of the Yellow River Basin has been continuously improved during the study period (Table 2; Fig. 3). Zones with the slight decrease of vegetation NDVI had the second largest area, which accounted for 30.820% of the total basin area, while zones with the intensive increase of vegetation NDVI only accounted for 0.012% of the total basin area. These results showed that the vegetation condition was improved in 68.080% of the total basin area, while it was degraded in 31.920% of the whole study region.

3.3 Distribution characteristics and migration of the gravity centers of vegetation NDVI during 1981–2019

The gravity center model can more vividly and intuitively reflect the spatial and temporal patterns and gravity centers deviations of vegetation coverage change in the Yellow River Basin. This study utilized the gravity center model to explore the spatial distribution of vegetation NDVI change at different time scales (1, 5 and 10 a) from 1981 to 2019, and then used the standard deviation ellipse to reveal and determine the change position and migration trend of the gravity centers of vegetation NDVI during the study period. Taking the gravity centers of average vegetation NDVI during 1981–2019 as the origin, the distance (radius) and offset angle

Table 2 Area proportions of different levels of Normalized Difference Vegetation Index (NDVI) change intensity in the Yellow River Basin during 1981–2019

Change intensity		Area (km^2)	Proportion (%)
Level	Value		
Intensive decrease	–0.9 to –0.6	208.00	0.026
Moderate decrease	–0.6 to –0.3	8533.00	1.072
Slight decrease	–0.3–0.0	245,233.00	30.820
Slight increase	0.0–0.3	507,960.00	63.830
Moderate increase	0.3–0.6	33,741.00	4.240
Intensive increase	0.6–0.9	95.00	0.012

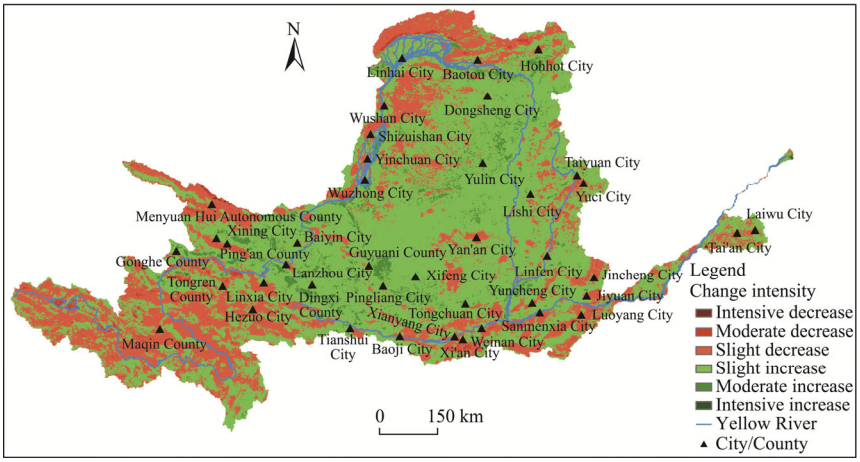

Fig. 3 Spatial distribution of different levels of NDVI change intensity in the Yellow River Basin during 1981–2019

(polar angle) to the origin were calculated to intuitively reflect the migration direction and distance of the gravity centers.

As shown in Figure 4a1 and a2, the gravity centers of vegetation NDVI were mostly located in the junction zone of Zhenyuan County and Huanxian County in Gansu Province and Pengyang County in Ningxia Hui Autonomous Region at the 1-a scale. The area of the standard deviation ellipse was 494.14 km^2 (Table 3), and the gravity centers were distributed in the southwest–northeast direction. In polar coordinates, the gravity centers of the southwest quadrant accounted for the largest proportion, followed by those of the northeast quadrant. The gravity centers of the northwest and southeast quadrants accounted for a relatively small proportion. The proportion of the gravity centers in the southern half was higher than that in the northern half, indicating that the increment and growth rate of vegetation NDVI in the southern half were larger than those in the northern half.

At the 5-a scale, the area of the standard deviation ellipse was 251.76 km^2, and the distribution of the gravity centers was relatively discrete (Fig. 4b1 and b2). In polar coordinates, the gravity centers were unevenly distributed, among which the southwest quadrant had the largest proportion of the gravity centers, followed by the northeast quadrant. Moreover, at the 10-a scale, the area of the standard deviation ellipse was 169.62 km^2 (Fig. 4c1 and c2). In polar coordinates, the gravity centers of vegetation NDVI in the Yellow River Basin were mainly concentrated in the southeast quadrant during 1981–2010, while the gravity centers of vegetation NDVI were distributed in the northeast quadrant during 2010–2019.

In order to further reveal the change law of the gravity centers of vegetation NDVI in the study area, this study explored the migration trajectory of the gravity centers at the 5-, 10- and 20-a scales. During 1981–1995, the gravity centers of vegetation NDVI migrated to the

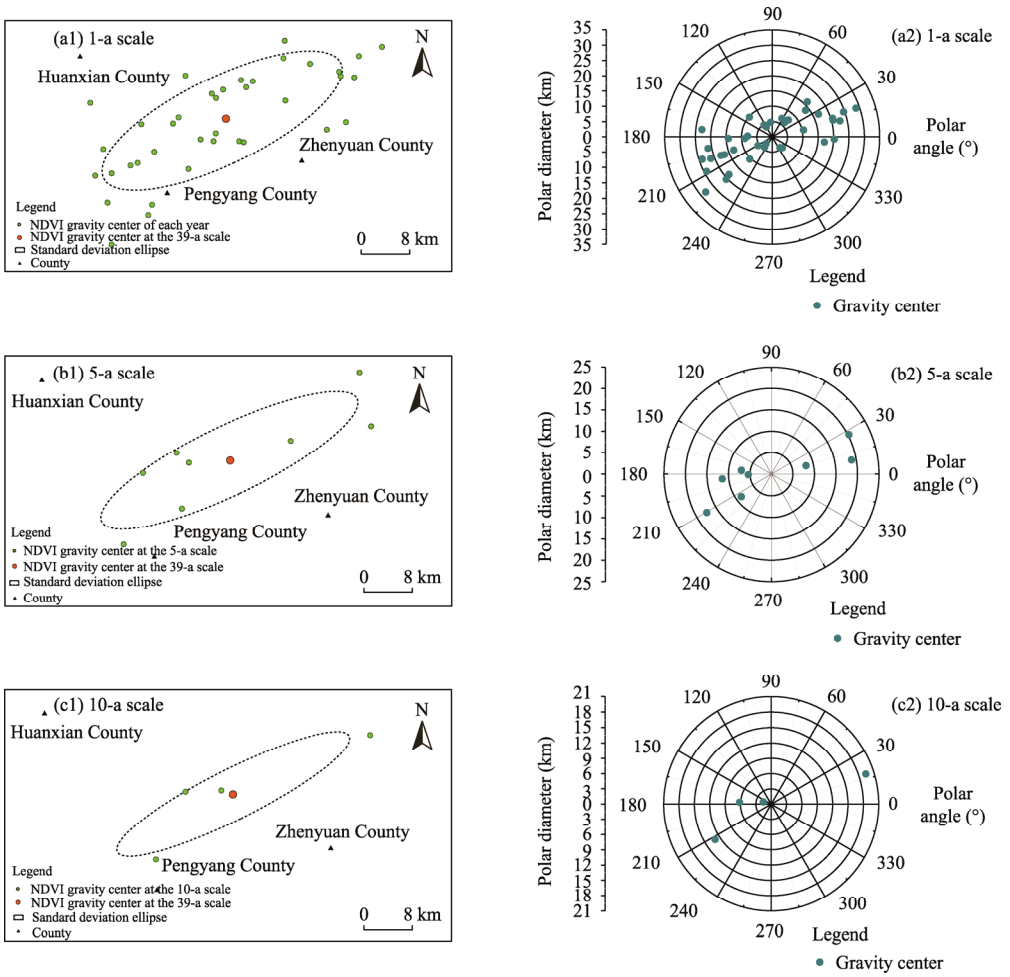

Fig. 4 Spatial distribution (a1, b1 and c1) and polar coordinates (a2, b2 and c2) of the gravity centers of vegetation NDVI in the Yellow River Basin at the 1-, 5- and 10-a scales during 1981–2019

Table 3 Standard deviation elliptic parameters of the gravity centers of vegetation NDVI in the Yellow River Basin during 1981–2019

Standard deviation elliptic parameter	Time scale		
	1 a	5 a	10 a
Polar angle (°)	71.01	70.84	69.81
Polar diameter along the *X* axis (km)	0.07	0.04	0.03
Polar diameter along the *Y* axis (km)	0.24	0.20	0.18
Area of the standard deviation ellipse (km^2)	494.14	251.76	169.62

northeast at the 5-a scale (Fig. 5a), indicating that the increment and growth rate of vegetation NDVI in the northeastern part were greater than those in the southwestern part. During 1991–2006, the migration trajectory of the gravity centers of vegetation NDVI showed a triangular trend of 'northwest–southwest–northeast'. The gravity centers migrated to the northeast during 2001–2015. Compared with the situation during 2001–2015, the gravity centers of vegetation NDVI during 2016–2019 moved to the northwest. The migration distance of the gravity centers of vegetation NDVI was the largest during the periods from 2001–2005 to 2006–2010, at the value of 19.40 km. During the periods from 1991–1995 to 1996–2000, the migration distance of the gravity centers of vegetation NDVI was the smallest, with the value of only 2.01 km. In general, the gravity centers of vegetation NDVI during 1981–2019 showed a moving trend of

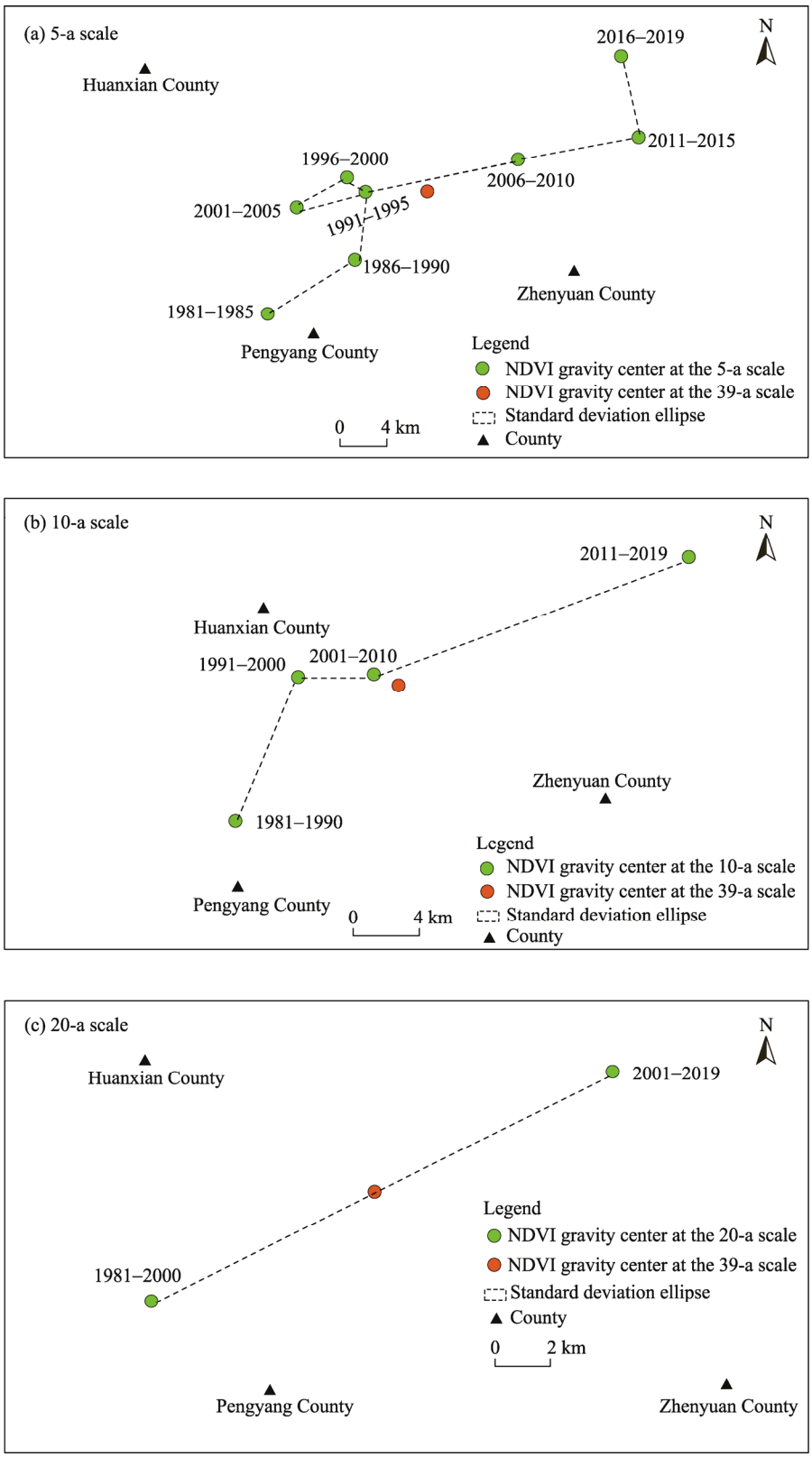

Fig. 5 Migration trajectory of the gravity centers of vegetation NDVI in the Yellow River Basin at different time scales during 1981–2019. (a), 5-a scale; (b), 10-a scale; (c), 20-a scale.

"northward→eastward→northward", indicating that the increment and growth rate of vegetation NDVI in the northern and eastern parts of the study area were greater than those in the southern and western parts.

As shown in Figure 5b, at the 10-a scale, the gravity centers of vegetation NDVI moved to northeastward with a mitigation distance of 9.31 km from 1991–1990 to 1991–2000. During the periods from 1991–2000 to 2001–2010, the gravity centers moved to eastward with the smallest mitigation distance of 4.60 km. During the periods from 2001–2010 to 2011–2019, the gravity centers moved to the northeast, with the largest migration distance of 20.37 km. During the study period (1991–2019), the gravity centers of vegetation NDVI were located in Qingyang City, Gansu Province. On the whole, the gravity centers of vegetation NDVI showed a moving trend of "northeastward→eastward→northeastward". The moving distance in the north–south direction was smaller than that in the east–west direction, indicating that the increment and growth rate of the gravity centers of vegetation NDVI in the northeast direction during this period were higher than those in the southwest direction.

During the periods from 1991–2000 to 2001–2019, the gravity centers of vegetation NDVI migrated to the northeast with a distance of 20.24 km at the 20-a scale (Fig. 5c), indicating that the increment and growth rate of vegetation NDVI in Gansu Province were higher than those in Ningxia Hui Autonomous Region during 1991–2019.

3.4 Relative action distinctions of climate change and human activities on vegetation NDVI change

As shown in Figure 6, during the study period, the correlation coefficients between $NDVI_{climate}$ and $NDVI_{actural}$ ranged from 0.65 to 0.91, with the average value of 0.85, which indicated that the inversed $NDVI_{climate}$ had higher applicability for the further study.

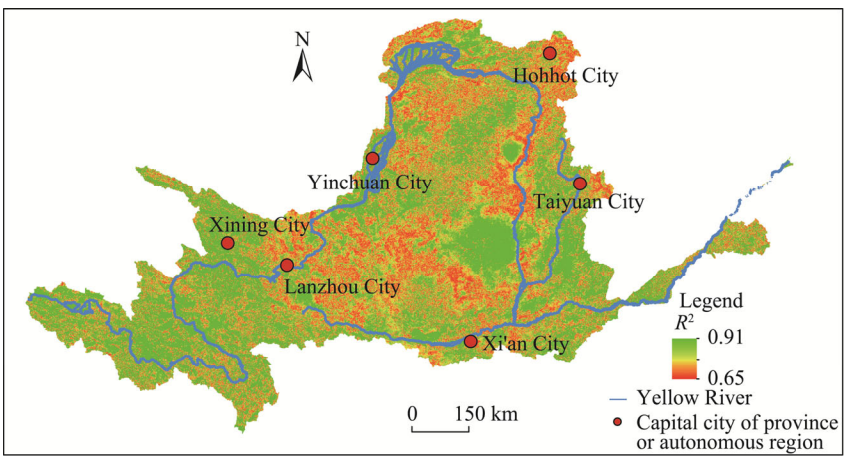

Fig. 6 Spatial distribution of the correlation coefficient (R^2) values between $NDVI_{climate}$ and $NDVI_{actural}$ in the Yellow River Basin during 1981–2019. $NDVI_{climate}$ is the predicted vegetation NDVI value by regression analysis, which is the action result of climate change; and $NDVI_{actual}$ is the observed vegetation NDVI value by remote sensing images, which is the result of the combined action of climate change and human activities.

Figure 7 showed that during 1981–2000, vegetation restoration areas were mostly located in the central and northern parts and downstream areas of the Yellow River Basin, including northern Gansu Province, Ningxia Hui Autonomous Region, southern Inner Mongolia Autonomous Region, Shaanxi Province and northern Shanxi Province. Vegetation degradation areas were mainly located in the western, southern and eastern parts of the Yellow River Basin, including Qinghai Province, western Gansu Province, central and southern Shaanxi Province and Shanxi Province, and Henan Province. In general, the area proportion of vegetation restoration was larger than that of vegetation degradation. Zones of vegetation restoration promoted by the combined action of climate change and human activities had the largest area

proportion (32.710%), mainly distributed in Lanzhou City in northern Gansu Province, Yulin City in northern Shaanxi Province, Xinzhou City in northwestern Shanxi Province and southeastern Ordos City in Inner Mongolia Autonomous Region. On the contrary, zones of vegetation restoration promoted by climate change had smallest area proportion (4.960%), mainly distributed in Shaanxi Province and southwestern Shanxi Province.

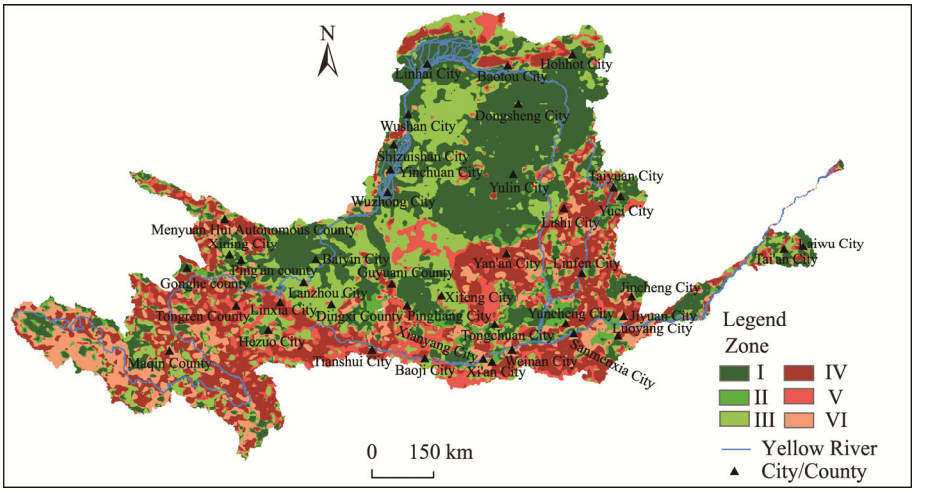

Fig. 7 Relative action distinctions of climate change and human activities on vegetation evolution in the Yellow River Basin during 1981–2000. I, vegetation restoration promoted by the combined action of climate change and human activities; II, vegetation restoration promoted by climate change; III, vegetation restoration promoted by human activities; IV, vegetation degradation induced by the combined action of climate change and human activities; V, vegetation degradation induced by climate change; VI, vegetation degradation induced by human activities.

During 2001–2019, vegetation restoration areas were mainly located in the central part of the study area, including the western Gansu Province, Ningxia Hui Autonomous Region, southern Inner Mongolia Autonomous Region, central and northern Shaanxi Province and Shanxi Province (Fig. 8). In contrast, vegetation degradation areas were mainly concentrated in the western parts of the Yellow River Basin, including Qinghai Province and western Gansu Province. Zones of vegetation restoration promoted by the combined action of climate change and human activities had the largest area proportion (40.840%), mainly distributed in Yulin City and Yan'an City in Shaanxi Province, Lvliang City, Linfen City and Yuncheng City in Shanxi Province, and southeastern Ordos City in Inner Mongolia Autonomous Region. On the contrary, zones of vegetation restoration promoted by climate change had smallest area proportion, at 1.370%. Compared with 1981–2000, the proportion of vegetation restoration areas promoted by the combined action of climate change and human activities and by human activities increased during 2001–2019, indicating that human activities had played a more important role in vegetation restoration during this period.

3.5 Dominant factors of vegetation evolution in different historical periods

3.5.1 Single factor

A factor detector was applied to detect and reveal the contribution rate (explanatory power) of each single factor to vegetation evolution in the Yellow River Basin during 1981–2019 (Table 4).

In 1981, the explanatory power of the single factor was ranked as follows: sunshine hours> precipitation>temperature>altitude>slope>population intensity>GDP intensity>aspect. Sunshine hours, precipitation and temperature were the dominant factors affecting vegetation NDVI in the Yellow River Basin, with the q values of 0.676, 0.679 and 0.696, respectively. The explanatory power of human activity factors including population intensity and GDP intensity was smaller, with the q values of 0.348 and 0.334, respectively.

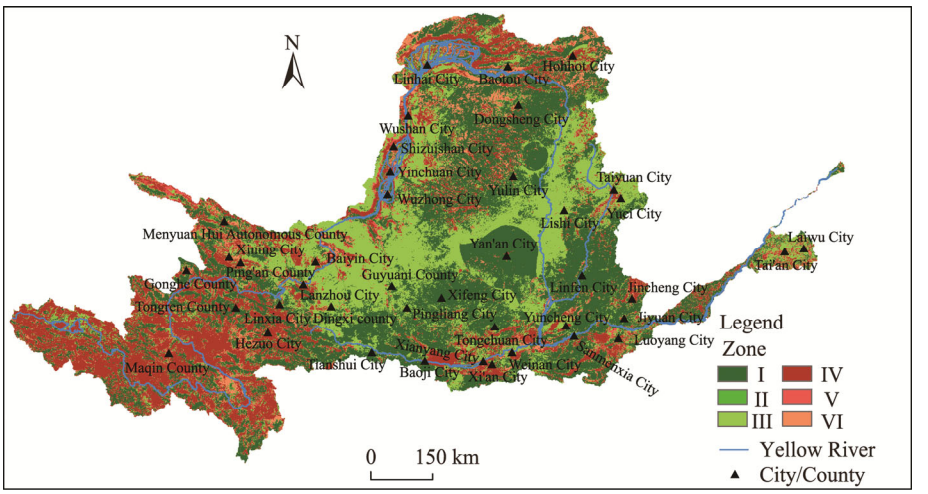

Fig. 8 Relative action distinctions of climate change and human activities on vegetation evolution in the Yellow River Basin during 2001–2019

Table 4 Explanatory power of the single factor on vegetation evolution in the Yellow River Basin in different years from 1981 to 2019

Single factor	*q* value			
	1990	2000	2010	2019
Altitude	0.512	0.514	0.557	0.467
Aspect	0.107	0.107	0.109	0.108
Slope	0.445	0.422	0.446	0.455
Population intensity	0.348	0.353	0.318	0.680
GDP intensity	0.334	0.341	0.330	0.692
Temperature	0.676	0.619	0.655	0.689
Precipitation	0.679	0.715	0.652	0.655
Sunshine hours	0.696	0.577	0.702	0.673

Note: The correlation degree is represented by the *q* value, and the explanatory power of a factor to vegetation NDVI is revealed.

In 2000, the explanatory power of the single factor was ranked as follows: precipitation> temperature>sunshine hours>altitude>slope>population intensity>GDP intensity>aspect. Precipitation and temperature were the dominant factors affecting vegetation NDVI, with the *q* values of 0.715 and 0.619, respectively. The explanatory power of population intensity and GDP intensity was smaller, with the *q* values of 0.353 and 0.341, respectively. The explanatory power of aspect was the smallest, with the *q* value of 0.107.

In 2010, the explanatory power of the single factor was ranked as follows: sunshine hours> temperature>precipitation>altitude>slope>GDP intensity>population intensity>aspect. Sunshine hours and temperature had the largest explanatory power for vegetation NDVI, with the *q* values of 0.702 and 0.655, respectively. Population intensity and GDP intensity had smaller contribution rates to vegetation evolution, with the *q* values of 0.318 and 0.330, respectively.

In 2019, the explanatory power of the single factor to vegetation evolution was ranked as follows: GDP intensity>temperature>population intensity>sunshine hours>precipitation>altitude> slope>aspect. GDP intensity, temperature and population intensity were the dominant factors affecting vegetation evolution in the Yellow River Basin, with the *q* values of 0.692, 0.689 and 0.680, respectively. The explanatory power of altitude and slope on vegetation evolution in the Yellow River Basin was smaller, with the *q* values of 0.467 and 0.455, respectively. The explanatory power of aspect on vegetation evolution was still the smallest, with the *q* value of 0.108.

3.5.2 Interactive factors

Interaction detection was applied to quantitatively evaluate the interactions among different influencing factors on vegetation NDVI, and the analysis of the interactions among various influencing factors was conductive to further study the driving mechanism of vegetation coverage change. The results shown in Figure 9 indicated that the q values of the interactive factors were larger than those of the single factor, implying that the influence process of factors on vegetation NDVI was not independent, but a mutual enhancement process.

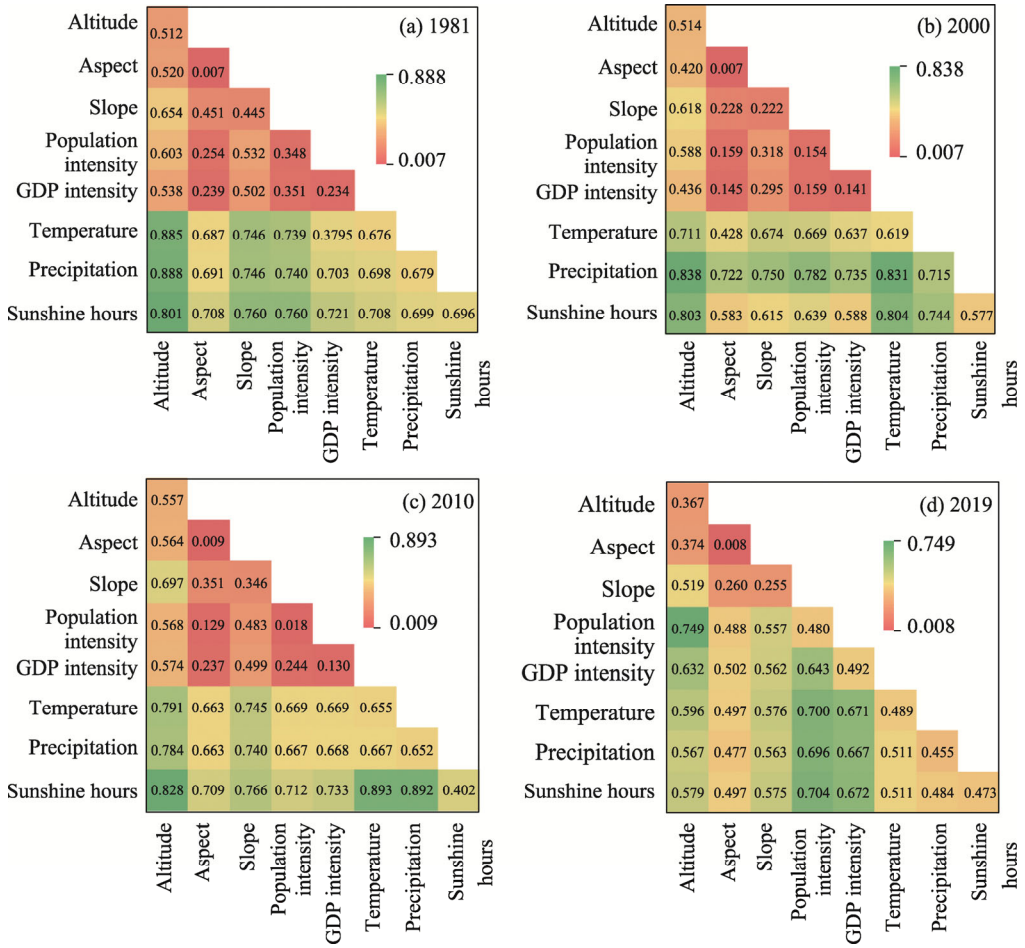

Fig. 9 Factor interaction detection of vegetation NDVI changes in the Yellow River Basin in 1981 (a), 2000 (b), 2010 (c) and 2019 (d)

The interactive factors with higher explanatory power in 1981 were as follows: altitude∩precipitation (q=0.888)>altitude∩temperature (q=0.885)>altitude∩sunshine hours (q=0.801)>slope∩sunshine hours (q=0.760)=population intensity∩sunshine hours (q=0.760)>slope∩temperature (q=0.746) (Fig. 9a). The explanatory power of altitude∩other factors was higher, while that of interactions among population intensity, GDP intensity and aspect was lower. The q value of aspect∩aspect was the smallest, at 0.007.

The interactive factors with higher explanatory power in 2000 were as follows: altitude∩precipitation (q=0.838)>temperature∩precipitation (q=0.831)>temperature∩sunshine hours (q=0.804)>altitude∩sunshine hours (q=0.803)>population intensity∩precipitation (q=0.782)>slope∩precipitation (q=0.750) (Fig. 9b). The explanatory power of altitude∩precipitation was the highest, while the explanatory power of aspect∩aspect was the lowest.

The interactive factors with higher explanatory power in 2010 were as follows: temperature∩

sunshine hours (q=0.893)>precipitation∩sunshine hours (q=0.892)>altitude∩sunshine hours (q= 0.828)>altitude∩temperature (q=0.791)>altitude∩precipitation (q=0.784)>slope∩sunshine hours (q=0.766) (Fig. 9c). The explanatory power of sunshine hours∩other factors was the largest, indicating that during this period, the variable of sunshine hours was the dominant factor affecting the change process of vegetation NDVI in the Yellow River Basin.

The interactive factors with higher explanatory power in 2019 were as follows: altitude∩population intensity (q=0.749)>population intensity∩sunshine hours (q=0.704)>population intensity∩temperature (q=0.700)>population intensity∩precipitation (q=0.696)>GDP intensity∩sunshine hours (q=0.672)>GDP intensity∩temperature (q=0.671) (Fig. 9d). The explanatory power of altitude∩population intensity was the largest, indicating that the influence of human activity factors on vegetation NDVI in this period was dominated.

4 Discussion

Spatial distribution of vegetation NDVI was the result of the combined effect of natural factors and human activities (Lu et al., 2020; Garioud et al., 2021). In the Yellow River Basin, zones with higher vegetation NDVI were concentrated in Huangnan Tibetan Autonomous Prefecture in western Qinghai Province and Gannan Tibetan Autonomous Prefecture in Gansu Province. The reason was that these areas are located in the Three River Source Regions with rich water resources, complex terrain and diverse landforms. In addition, with high altitude and low intensity of human activities, the ecological quality of these regions is better (Ferreira et al., 2020; Deng et al., 2021).

Vegetation NDVI in most of the upper reaches of the Yellow River was lower due to the serious desertification and soil erosion (Berzaghi et al., 2020). In addition, these regions belonged to semi-arid and arid areas with scare precipitation and frequent drought (Han et al., 2009; Jacques and Pienitz, 2022; Xu et al., 2022). Moreover, before 2000, human activities such as deforestation and overgrazing have exacerbated grassland degradation and desertification (Han et al., 2009). The average NDVI in the lower reaches of the Yellow River was higher, due to the fact that these regions were dominated by a temperate monsoon climate with abundant precipitation (Chen et al., 2021).

During 1981–2019, the gravity centers of vegetation NDVI in the Yellow River Basin moved northeastwards, indicating that the increment and growth rate of vegetation coverage in the northeastern part were greater than those in the other regions (Kumar and Scheiter, 2019; Guo et al., 2022b). The reason was that since 2000, due to the implementation of policies such as returning farmland to forest, returning grazing pastures to grassland, and soil erosion control, the ecological environment quality of the Yellow River Basin was gradually improved (Xing et al., 2018; Li et al., 2020). Moreover, the warm and humid climate in Northeast China was more conducive to the growth of vegetation, so that the gravity centers of vegetation NDVI shifted to the northeast.

In 1981, the interactive dominant factor on vegetation NDVI was altitude∩precipitation, while in 2019, the interactive dominant factor changed greatly, with altitude∩population intensity being the interactive dominant factor. Before 2000, human activities such as overgrazing and the reclamation of steep slopes had exacerbated the degradation of grassland and regional desertification. Since 2000, the prohibition of deforestation, the implementation of the project of returning farmland to forest (grassland) and the continuous adjustment of land use structure had promoted the growth of forest vegetation. All in all, vegetation coverage in the Yellow River Basin had been continuously improved in recent years (Garzanti et al., 2022).

5 Conclusions

Based on the climate data, GIMMS NDVI and MODIS NDVI data in the Yellow River Basin from 1981 to 2019, this study investigated the spatial and temporal evolution patterns of

vegetation NDVI, quantitatively distinguished the relative actions of climate change and human activities on vegetation evolution, and clarified the dominant factors influencing vegetation evolution in different historical periods.

At the spatial scale, there was a decreasing trend of vegetation NDVI in the Yellow River Basin from southeast to northwest; at the temporal scale, vegetation NDVI showed an overall increasing trend from 1981 to 2019. The gravity centers of average vegetation NDVI during 1981–2019 was distributed in Zhenyuan County, Gansu Province, and the gravity centers moved northeastwards over the course during this period. During 1981–2000 and 2001–2019, the area proportion of vegetation restoration promoted by the combined action of climate change and human activities was the largest. During 1981–2019, the dominant single factor affecting the temporal and spatial evolution patterns of vegetation NDVI in the Yellow River Basin shifted from sunshine hours and precipitation (1981) to GDP intensity and temperature (2019), while the dominant interactive factor shifted from altitude∩precipitation (1981) to altitude∩population intensity (2019), indicating that the contribution of human activities in the process of vegetation evolution was increasing.

Acknowledgements

This work was supported by grants from the National Natural Science Foundation of China (42101306, 4217107), the Natural Science Foundation of Shandong Province (ZR2021MD047), the Strategic Priority Research Program of the Chinese Academy of Sciences (XDA2002040203), the Open Fund of the Key Laboratory of National Geographic Census and Monitoring, Ministry of Natural Resources (MNR) (2020NGCM02), the Open Fund of the Key Laboratory of Urban Land Resources Monitoring and Simulation, Ministry of Natural Resources (KF-2020-05-001), and the Major Project of the High Resolution Earth Observation System of China (GFZX0404130304).

References

Agatova A R, Nepop R K, Carling P A, et al. 2020. Last ice-dammed lake in the Kuray basin, Russian Altai: New results from multidisciplinary research. Earth-Science Reviews, 205: 103183, doi: 10.1016/j.earscirev.2020.103183.

Amundson R, Heimsath A, Owen J, et al. 2015. Hillslope soils and vegetation. Geomorphology, 234: 122–132.

Berzaghi F, Wright I J, Kramer K, et al. 2020. Towards a new generation of trait-flexible vegetation models. Trends in Ecology & Evolution, 35(3): 191–205.

Chen C, Wang Y M, Li Y Y, et al. 2022. Vegetation changes and influencing factors in different climatic regions of Yellow River basin from 1982 to 2015. Journal of Yangtze River Scientific Research, 39(2): 56–62, 81. (in Chinese)

Chen S T, Guo B, Zhang R, et al. 2021. Quantitatively determine the dominant driving factors of the spatial–temporal changes of vegetation NPP in the Hengduan Mountain area during 2000–2015. Journal of Mountain Science, 18(2): 427–445.

Dai L, Zhang L, Wang K, et al. 2014. Vegetation changing trend and its affecting factors in Mongolian Plateau. Bulletin of Soil and Water Conservation, 34(5): 218–225. (in Chinese)

Deng C N, Liu L S, Li H S, et al. 2021. A data-driven framework for spatiotemporal characteristics, complexity dynamics, and environmental risk evaluation of river water quality. Science of The Total Environment, 785: 147134, doi: 10.1016/j.scitotenv.2021.147134.

Duo A, Zhao W J, Qu X Y, et al. 2016. Spatio-temporal variation of vegetation coverage and its response to climate change in North China plain in the last 33 years. International Journal of Applied Earth Observation and Geoinformation, 53: 103–117.

Fang L L, Wang L C, Chen W X, et al. 2021. Identifying the impacts of natural and human factors on ecosystem service in the Yangtze and Yellow River Basins. Journal of Cleaner Production, 314: 127995, doi: 10.1016/j.jclepro.2021.127995.

Ferreira V G, Yong B, Tourian M J, et al. 2020. Characterization of the hydro-geological regime of Yangtze River basin using remotely-sensed and modeled products. Science of The Total Environment, 718: 137354, doi: 10.1016/j.scitotenv.2020.137354.

Garioud A, Valero S, Giordano S, et al. 2021. Recurrent-based regression of Sentinel time series for continuous vegetation monitoring. Remote Sensing of Environment, 263: 112419, doi: 10.1016/j.rse.2021.112419.

Garzanti E, Capaldi T, Tripaldi A, et al. 2022. Andean retroarc-basin dune fields and Pampean Sand Sea (Argentina): Provenance and drainage changes driven by tectonics and climate. Earth-Science Reviews, 231: 104077, doi: 10.1016/j.earscirev.2022.104077.

Guo B, Zang W Q, Luo W. 2020a. Spatial-temporal shifts of ecological vulnerability of Karst Mountain ecosystem-impacts of global change and anthropogenic interference. Science of The Total Environment, 741: 140256, doi: 10.1016/j.scitotenv.2020.140256.

Guo B, Zang W Q, Yang F, et al. 2020b. Spatial and temporal change patterns of net primary productivity and its response to climate change in the Qinghai-Tibet Plateau of China from 2000 to 2015. Journal of Arid Land, 12(1): 1–17.

Guo B, Wei C X, Yu Y, et al. 2022a. The dominant influencing factors of desertification changes in the source region of Yellow River: climate change or human activity? Science of The Total Environment, 813: 152512, doi: 10.1016/j.scitotenv.2021.152512.

Guo B, Yang F, Fan J F, et al. 2022b. The changes of spatiotemporal pattern of rocky desertification and its dominant driving factors in typical karst mountainous areas under the background of global change. Remote Sensing, 14(10): 2351, doi: 10.3390/rs14102351.

Han H H, Yang T B, Wang Y L. 2009. Land use and landscape pattern change in Guinan County of Qinghai Province in recent 30 years. Progress in Geography, 28(2): 207–215. (in Chinese)

Hou Q Q, Pei T T, Yu X J, et al. 2022. The seasonal response of vegetation water use efficiency to temperature and precipitation in the Loess Plateau, China. Global Ecology and Conservation, 33: e01984, doi: 10.1016/j.gecco.2021.e01984.

Jacques O, Pienitz R. 2022. Asbestos mining waste impacts on the sedimentological evolution of the Bécancour chain of lakes, southern Quebec (Canada). Science of The Total Environment, 807(3): 151079, doi: 10.1016/j.scitotenv.2021.151079.

Jiang H L, Sun X H, Yao Z Y, et al. 2021. Formation of lake dunes in an intramontane basin: A case study from Cuona Lake, on the Qinghai-Tibetan Plateau. Aeolian Research, 52: 100715, doi: 10.1016/j.aeolia.2021.100715.

Kumar D, Scheiter S. 2019. Biome diversity in South Asia-How can we improve vegetation models to understand global change impact at regional level? Science of The Total Environment, 671: 1001–1016.

Li J G, Vandenberghe J, Mountney N P, et al. 2020. Grain-size variability of point-bar deposits from a fine-grained dryland river terminus, Southern Altiplano, Bolivia. Sediment Geology, 403: 105663, doi: 10.1016/j.sedgeo.2020.105663.

Li Q Q, Cao Y P, Miao S L. 2022. Spatial and temporal changes of vegetation in the Yellow River Basin and its response to climatic factors. Acta Ecologica Sinica, 42(10): 4041–4054. (in Chinese)

Liu H, Liu F, Zheng L. 2021. Effects of climate change and human activities on vegetation cover change in the Yellow River Basin. Journal of Soil and Water Conservation, 35(4): 143–151. (in Chinese)

Lu J, Wang X F, Cao Y Q. 2022. Effects of climate and human activities on vegetation variation in Liaoning Province. Advances in Science and Technology of Water Resources, 42(4): 7–14, 38. (in Chinese)

Lu Q, Liu G L, Yan B, et al. 2021. Variation of extreme precipitation events and their impacts on vegetation coverage in central Asia under climate warming. Research of Soil and Water Conservation, 28(4): 226–235. (in Chinese)

Lu Q Q, Jiang T, Liu D L, et al. 2020. The response characteristics of NDVI with different vegetation cover types to temperature and precipitation in China. Ecology and Environment Sciences, 29(1): 23–34. (in Chinese)

Meng X, Kooijman A M, Temme A J A M, et al. 2022. The current and future role of biota in soil-landscape evolution models. Earth-Science Reviews, 226: 103945, doi: 10.1016/j.earscirev.

Morgan B E, Chipman J W, Bolger D T. 2020. Spatiotemporal analysis of vegetation cover change in a large Ephemeral River: multi-sensor fusion of Unmanned Aerial Vehicle (UAV) and Landsat imagery. Remote Sensing, 13(1): 12457–12468.

Oakley N S, Cannon F, Boldt E, et al. 2018. Origins and variability of extreme precipitation in the Santa Ynez River Basin of Southern California. Journal of Hydrology: Regional Studies, 19: 164–176.

Qu S, Wang L C, Lin A W, et al. 2020. Distinguishing the impacts of climate change and anthropogenic factors on vegetation dynamics in the Yangtze River Basin, China. Ecological Indicators, 108: 105724, doi: 10.1016/j.ecolind.2019.105724.

Sidi A M A, Wu Y P, Kumar A. 2021. Spatiotemporal analysis of vegetation cover changes around surface water based on NDVI: a case study in Korama basin, Southern Zinder, Niger. Applied Water Science, 11(1): 568–579.

Stecca G, Fedrizzi D, Measures R, et al. 2022. Development of a numerical model for braided river morphology and vegetation evolution with application to the Lower Waitaki River (Aotearoa – New Zealand). Advances in Water Resources, 166: 104236, doi: 10.1016/j.advwatres.2022.104236.

Tardy Y, Bustillo V, Roquin C, et al. 2005. The Amazon. Bio-geochemistry applied to river basin management Part I. Hydro-

climatology, hydrograph separation, mass transfer balances, stable isotopes, and modelling. Applied Geochemistry, 20(9): 1746–1829.

Twilley R R, Day J W, Bevington A E, et al. 2019. Ecogeomorphology of coastal deltaic floodplains and estuaries in an active delta: Insights from the Atchafalaya Coastal Basin. Eatuarine Coastal and Shelf Science, 227: 106341, doi: 10.1016/j.ecss.2019.106341.

Wang X L, Shi S H, Chen J Z X. 2022. Study on vegetation coverage change and driving factors in the Yellow River Basin. China Environmental Science, doi: 10.19674/j.cnki.issn1000-6923.20220712.002. (in Chinese)

Wang Z Y, Wang G Q, Huang G H. 2008. Modeling of state of vegetation and soil erosion over large areas. International Journal of Sediment Research, 23(3): 181–196.

Wu D H, Wu H, Zhao X. 2014. Evaluation of spatiotemporal variations of global fractional vegetation cover based on GIMMS NDVI data from 1982 to 2011. Remote Sensing, 6(5): 4217–4239, doi: 10.3390/rs6054217.

Wu H W, Guo B, Fan J F, et al. 2021. A novel remote sensing ecological vulnerability index on large scale: A case study of the China-Pakistan Economic Corridor region. Ecological Indicators, 129: 107955, doi: 10.1016/j.ecolind.2021.107955.

Wu Q S, Zuo Q T, Han C H, et al. 2022. Integrated assessment of variation characteristics and driving forces in precipitation and temperature under climate change: A case study of Upper Yellow River basin, China. Atmospheric Research, 272: 106156, doi: 10.1016/j.atmosres.2022.106156.

Xing W Q, Wang W G, Zou S, et al. 2018. Projection of future runoff change using climate elasticity method derived from Budyko framework in major basins across China. Global Planet Change, 162: 120–135.

Xu S Y, Fu P, Quincey D C, et al. 2022. UAV-based geomorphological evolution of the Terminus Area of the Hailuogou Glacier, Southeastern Tibetan Plateau between 2017 and 2020. Geomorphology, 411: 108293, doi: 10.1016/j.geomorph.2022.108293.

Yi L, Ren Z Y, Zhang C, et al. 2014. Relationship between vegetation cover change and climate and human activity in the Loess Plateau. Resource Science, 36(1): 166–174. (in Chinese)

Yuan L Y, Gao Y C, Cheng F Y, et al. 2022. The influence of oil exploitation on the degradation of vegetation: A case study in the Yellow River Delta Nature Reserve, China. Environment Technology & Innovation, 28: 102579, doi: 10.1016/j.eti.2022.102579.

Zhang C Y. 2022. Study on monitoring the spatio-temporal dynamics of wetland vegetation in the Yellow River delta by remote sensing. Journal of East China Normal University, doi: 10.27149/d.cnki.ghdsu.2022.001705. (in Chinese)

Zhang H Y, Zhan C S, Xia J, et al. 2022. The role of groundwater in the spatio-temporal variations of vegetation water use efficiency in the Ordos Plateau, China. Journal of Hydrology, 605: 127332, doi: 10.1016/j.jhydrol.2021.127332.

Zhang Y H, Wang L, Jiang J, et al. 2022. Application of soil quality index to determine the effects of different vegetation types on soil quality in the Yellow River Delta wetland. Ecological Indicators, 141: 109116, doi: 10.1016/j.ecolind.2022.109116.

Zhao Y, Wang M. 2021. Empirical Analysis of Green GDP Accounting in China in the New Era. Tropical Agricultural Engineering, 45(5): 39–44. (in Chinese)

Zhong L, Ma Y M, Salama M S, et al. 2010. Assessment of vegetation dynamics and their response to variations in precipitation and temperature in the Tibetan Plateau. Climatic Change, 103: 519–535.

Zhu Q, Zhang H. 2022. Groundwater drought characteristics and its influencing factors with corresponding quantitative contribution over the two largest catchments in China. Journal of Hydrology, 609: 127759, doi: 10.1016/j.jhydrol.2022.127759.